

DC-DC Converter Control for Peak-Shaving in Shipboard DC Power System via Hybrid Control

Daeseong Park
Department of Marine Technology
Norwegian University of
Science and Technology
Trondheim, Norway
daeseong.park@ntnu.no

Mehdi Karbalaye Zadeh
Department of Marine Technology
Norwegian University of
Science and Technology
Trondheim, Norway
mehdi.zadeh@ntnu.no

Roger Skjetne
Department of Marine Technology
Norwegian University of
Science and Technology
Trondheim, Norway
roger.skjetne@ntnu.no

Abstract—For the stable operation of the shipboard hybrid DC power systems, the DC bus voltage should be controlled within the recommended range by the regulations. However, the challenge comes from the load variations, and it makes the main bus voltage fluctuate. This paper proposes a control approach based on hybrid dynamical modeling of the DC-DC converter for the battery interface. In this method, the switching signal of the DC-DC converter is calculated to satisfy the Lyapunov stability criteria, and the reference power of the battery is generated for the peak-shaving of the load changes to stabilize the voltage. The effectiveness of the controller is evaluated with real ship load data which has a transient profile. The performance of the proposed control strategy is presented, and the results show that the proposed method can provide significant advantages in terms of fast and stable control performance, as well as the peak-shaving function by the battery to operate the diesel generators at the best efficiency point.

Index Terms—DC-DC converter, hybrid dynamical system, peak-shaving, batteries, onboard DC power system, hybrid electric ships.

I. INTRODUCTION

Shipboard hybrid DC power systems which are combined with diesel generators (DGs) and energy storage systems (ESSs) have been proposed as an alternative propulsion system in the marine industry recently. Shipboard hybrid DC power system can be operated more economical and environmentally friendly over the AC systems because it is more flexible to integrate ESSs to the main grid as a power source. Then, the DGs can be operated optimally as a variable speed mode at each load level since the synchronization in frequency is not necessary. The variable speed operation can reduce the fuel oil consumption especially in low load operation and transient conditions, which is also related to lower operating cost and emissions. As aforementioned, the DC power system can easily integrate energy storage systems (ESSs) such as batteries, supercapacitors and fuel cells which are designed based on the DC system as shown in Fig. 1.

With the recent development of power electronics, the DC power system has been even more applicable, and they have been installed for the small ferries. The use of the ESSs can be operated with several operational functions. One of the modes is called peak-shaving that handles peak loads. Therefore, the sudden fast changes in the load can be compensated by

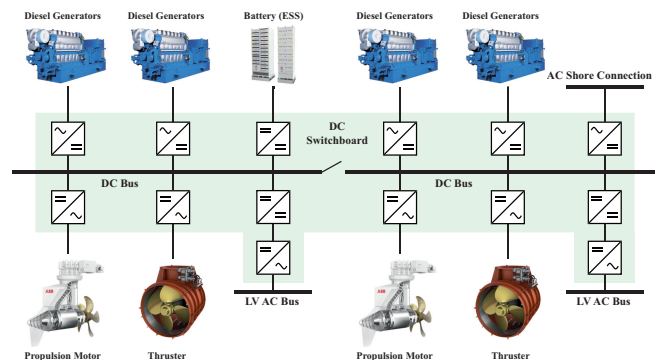


Fig. 1. A typical configuration of the shipboard hybrid DC power systems.

the ESSs while the DGs supply the filtered load with slow dynamics. The peak loads can come from fast changes in ship speed during maneuvering operations that involve switching between full-ahead and full-astern operation or in rough sea conditions. During this period, the voltages and current from the DGs can fluctuate and the combustion efficiency from the prime movers (diesel engines) can be worse due to the turbo-lag.

As a result, ESS can be used as a bank for such transient surge/load oscillations. Thanks to the fast response time, batteries or supercapacitors can be plausible candidates for the purpose of active mitigation methods against the transient conditions, as they are already used for peak-shaving that aims to smoothen the peak load and make the load of the DGs less erratic. The uses of the batteries are proposed to mitigate the voltage fluctuations in [1], [2]. Otherwise, the inertia of the DGs should compensate for load fluctuations but this operation can degrade the lifetime of the equipment in addition to the increased fuel consumption and emissions. Therefore, the peak-shaving operation by the battery is proposed in this study so that the fast dynamics can be handled the battery while the set-point of the DGs can be kept at their best efficiency points.

In the previous study [2], the main contribution is to calculate the power reference of the battery by using the model predictive control (MPC), but the control of the AC-DC converter for the battery interface to the AC grid is not

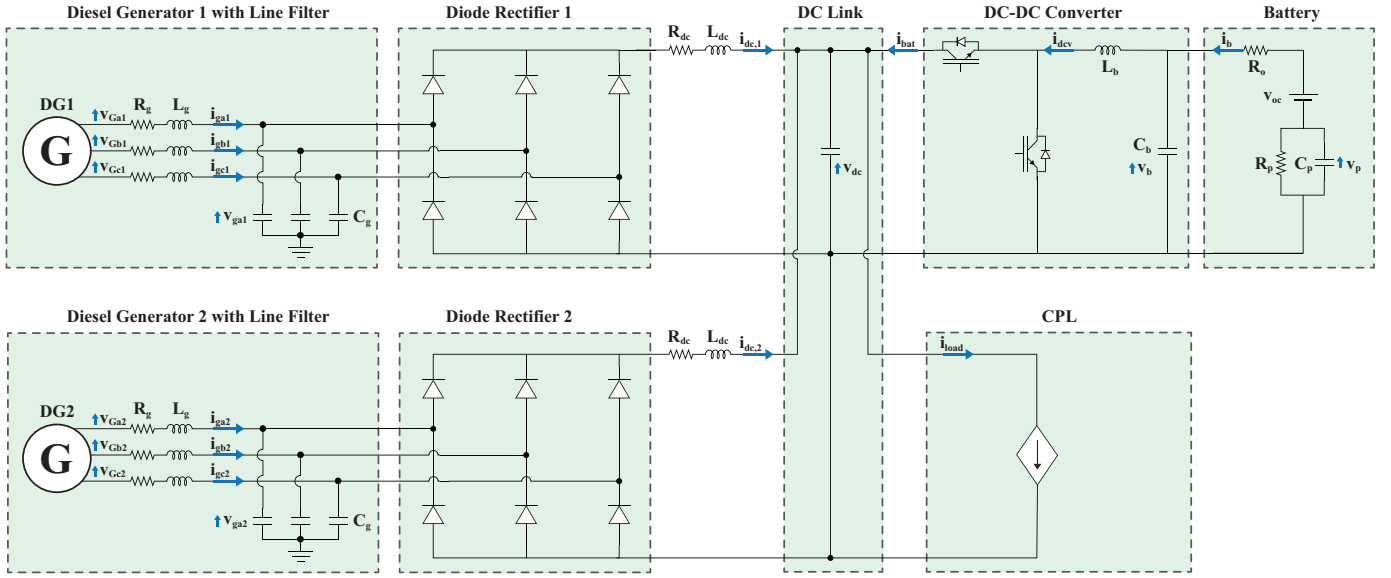


Fig. 2. Electric circuit diagram of the shipboard DC power system for the study.

considered. However, unlike the battery interface in the AC systems, ESSs are connected to the main DC grid through a DC-DC converter in the DC power systems, so it is required to control the voltage or current output of the DC-DC converter. This can be done by controlling Pulse Width Modulation (PWM) of the switches such as Metal Oxide Semiconductor Field-Effect Transistor (MOSFET) or Insulated Gate Bipolar Transistor (IGBT) in the converters. Therefore, the control of the DC-DC converter through the switching signal is the key to the peak shaving operation.

The control of the DC-DC converter is commonly done by proportional-integral (PI) controllers and MPC to control the output voltage and current by duty cycle calculation. Then, pulse-width modulation (PWM) technique is used to generate switching signals [3] to the switches. In addition to these methods, the DC-DC converter modeling and simulation via hybrid control has been done in [4]. The research focuses on controlling the boost converter to satisfy stability criteria at a given output voltage set-point. Consequently, the switching law is proposed to ensure the robust and global asymptotic

stability property. In this paper, it is aimed to build a bidirectional buck and boost DC-DC converter model based on hybrid dynamical system theory, and the control action is assigned to guarantee the Lyapunov stability criteria producing the current output for the peak-shaving. Therefore, PWM block is not used in this work, so variable switching frequency is applied to the controller of the DC-DC converter.

II. SHIPBOARD HYBRID DC POWER SYSTEM

In this section, the electric circuit diagram of the target shipboard DC power system is presented as seen in Fig. 2. The power system for the study consists of two three-phase generators, transmission lines, diode rectifiers, DC-filter (in DC-bus), a battery and a constant power load (CPL) to represent propulsion power loads which are tightly controlled by inverters.

The AC/DC conversion can be carried out diode rectifiers, thyristor rectifier or active front end rectifier [5], but the diode rectifier is used in this study for its wide usage in the industry. The diode rectifier can be modeled as a time-varying transformer in dq-frame so that the switching effect from the diode rectifier can be excluded in this study. Therefore, the rectifier has no control action to regulate the DC voltage through the rectifiers. Therefore, the main DC bus voltage is mainly regulated by an automatic voltage regulator (AVR) of the generators configured as a PI controller with a

TABLE I
MAIN PARAMETERS OF THE STUDIED ONBOARD DC POWER SYSTEM

Parameter	Unit	Value
v_G	V (rms)	690
f	Hz	60
R_g	m Ω	1
L_g	μ H	5
C_g	μ F	50
R_{dc}	m Ω	1
L_{dc}	μ H	5
C_{dc}	mF	50
$V_{dc,ref}$	V	1000
Sampling time (system)	μ s	10

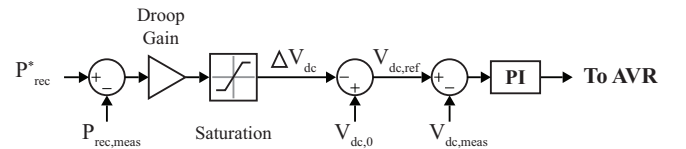


Fig. 3. DC droop for voltage control (Power-Voltage droop curve)

TABLE II
THE PARAMETERS FOR THE BATTERY AND DC-DC CONVERTER

Parameter	Unit	Value
v_{oc}	V	650
R_o	m Ω	50
R_p	m Ω	13
C_p	F	14300
$SOC_{t=0}$	pu	0.5
Rated capacity (battery)	Ah	500
L_b	mH	40
C_b	mF	1
Switching freq. (dc-dc)	kHz	1

voltage droop function (which is originally speed droop in AC systems) as shown in Fig. 3, so the battery supplies power only for the peak-shaving. The parameters for the main electrical components are listed in Table. I.

The battery and the DC-DC converter parameters are chosen as listed in Table. II. According to the sizing of the battery, it can produce 325 kW for an hour. The type of DC-DC converter in marine applications can be double stage with a high-frequency transformer to minimize the size and to ensure the isolation between the different voltage levels for safety. However, a half-bridge type of the DC-DC converter with multiple current paths is also widely used due to its simplicity, so the half-bridge type is selected (but with one current path) for this system-level analysis. Matlab/Simulink is used as a simulation tool for this work.

III. DYNAMIC MODELING OF THE SYSTEM WITH PREDICTIVE CONTROL

A. Diode rectifier

To formulate the controller, analytical equations of the system should be derived. First, for easier modeling of AC systems, the grid side voltages and currents are represented in dq-frame transformed from abc-frame of three phases by using Clarke and Park transform. This enables the dimension of the system to be reduced and the rectifiers to be represented as time-varying transformers [6] as aforementioned.

Then, for the rectifier, the switching function S_a of the diodes for a-phase as an example, can be represented by Fourier series as [7]:

$$S_a = \sum_{k=1,5,7,\dots}^{\infty} \frac{\sqrt{3}}{\pi} \frac{(-1)^{L+1}}{k} (-2 \sin(k\omega t)) \quad (1)$$

where $k = 6L \pm 1 (L = 0, 1, 2, \dots, k > 0)$

By considering only the fundamental component of the switching function ($k=1$), the voltage amplifying factor by the switching function of the rectifier can be determined as $2\sqrt{3}/\pi$. Then, by dq-transformation, the magnitude of the input current to the rectifier in dq-frame can be calculated as:

$$|i_{g,dq}| = \sqrt{\frac{3}{2}} \frac{2\sqrt{3}}{\pi} \cdot i_{dc} \quad (2)$$

B. Diesel generators with line filters

For the voltage from AC sources (v_{G1} and v_{G2}), we can define them as a simplified electrical representation of a pure sinusoidal source with a droop function.

Then, $i_{g,q}$ is set to be zero since the AC system is assumed to be balanced. For the integral calculation of $i_{dc,i}$, the factor for $v_{gd,i}$ is also same as $\sqrt{\frac{3}{2}} \frac{2\sqrt{3}}{\pi}$ because the power of the transformer at both sides should be equal. As a result, the equations for the synchronous machine (diesel generator) - rectifier systems can be given as:

$$\begin{aligned} L_g \frac{di_{gd,i}}{dt} &= v_{Gd,i} - R_g i_{gd,i} + \omega L_g i_{gq,i} - v_{gd,i} \\ L_g \frac{di_{gq,i}}{dt} &= v_{Gq,i} - R_g i_{gq,i} - \omega L_g i_{gd,i} - v_{gq,i} \\ C_g \frac{dv_{gd,i}}{dt} &= i_{gd,i} + \omega C_g v_{gq,i} - \sqrt{\frac{3}{2}} \frac{2\sqrt{3}}{\pi} i_{dc,i} \\ C_g \frac{dv_{gq,i}}{dt} &= i_{gq,i} - \omega C_g v_{gd,i} \\ L_{dc} \frac{di_{dc,i}}{dt} &= \sqrt{\frac{3}{2}} \frac{2\sqrt{3}}{\pi} v_{gd,i} - R_{dc} i_{dc,i} - v_{dc} \end{aligned} \quad (3)$$

As described in the electric circuit diagram in Figure 2, the DC voltage is calculated based on the Kirchoff's current law (KCL) as:

$$C_{dc} \frac{dv_{dc}}{dt} = \sum_i^2 i_{dc,i} + i_{bat} - \frac{P_M}{v_{dc}} \quad (4)$$

where,

- i Subscript index that denotes the number of bus
- P_M Required power of the propulsion motors as CPL (W)
- ω AC system frequency (rad/s)
- v_{Gdq} Voltage of diesel generator in dq-axis (V)
- i_{gdq} Diesel generator current in dq-axis (A)
- v_{gdq} Transmission line voltage in dq-axis (A)

Then, the states for the AC system and control inputs can be defined as $x_{AC} = [i_{gd,1} \ i_{gq,1} \ v_{gd,1} \ v_{gq,1} \ i_{dc,1} \ i_{gd,2} \ i_{gq,2} \ v_{gd,2} \ v_{gq,2} \ i_{dc,2} \ v_{dc}]^T$ and $u_{AC} = [v_{Gd,1} \ v_{Gq,1} \ v_{Gd,2} \ v_{Gq,2} \ i_{bat}]^T$. V_{Gd} and V_{Gq} are delivered from the AC source by the dq-transformation matrix, and i_{bat} is calculated from the control of the DC-DC converter. Therefore, V_{Gd} and V_{Gq} has slower dynamics than the states of the DC-DC converter, and it makes the AC voltage variations less dependent on hybrid control for the DC-DC converter. Only the battery current i_{bat} is made to be controlled by hybrid control in the later section.

C. DC-DC Converter

The DC-DC converter should be able to operate bidirectionally so that the battery can be charged from the DC grid and can discharge its power to the grid. The sign of the output current is defined as negative when the battery is charged and positive when the battery discharges. The analytical equations for each buck and boost mode can be expressed as:

Battery charging (buck mode) ($i_b, i_{dcv}, i_{bat} < 0$)

$$\begin{aligned} L_b \frac{di_{dcv}}{dt} &= v_b - qv_{dc} \\ C_b \frac{dv_b}{dt} &= i_b - i_{dcv} \\ i_{bat} &= qi_{dcv} \end{aligned} \quad (5)$$

Battery discharging (boost mode) ($i_b, i_{dcv}, i_{bat} > 0$)

$$\begin{aligned} L_b \frac{di_{dcv}}{dt} &= v_b - (1-q)v_{dc} \\ C_{dc} \frac{dv_{dc}}{dt} &= \sum_{i=1}^2 i_{dc,i} + i_{bat} - \frac{P_M}{V_{dc}} \\ i_{bat} &= (1-q)i_{dcv} \end{aligned} \quad (6)$$

q means the state of the switch, 1 for closed and 0 for opened. As seen in the equation above, it can be concluded that the number of equations can be reduced by having only one equation for each i_{dcv} and i_{bat} , if the states of the switches are chosen to be complementary such that the switches are not both opened or closed at the same time.

D. Battery

For the battery, Thévenin battery model is used to include transient behaviors of the battery [8]. Therefore, the battery parameters are kept constant during the whole simulation. The model consists of open-circuit voltage v_{ocv} , internal resistance R_o , and RC parallel circuit (R_p and C_p) to include the response to the load variations.

$$\begin{aligned} C_p \frac{dv_p}{dt} &= -\frac{v_p}{R_p} - i_b \\ v_b &= v_p - R_o i_b + v_{oc} \end{aligned} \quad (7)$$

Then, the current output from/to the battery can be calculated in (8), so SOC can be calculated by integrating the output current with respect to the sampling time as in (9).

$$i_b = \frac{v_p + v_{oc} - v_b}{R_o} \quad (8)$$

$$SOC = SOC(0) - \frac{1}{k_b Q_b} \int_0^t i_b dt \quad (9)$$

where $SOC(0)$ is the initial loading of the battery, k_b is 3600s and Q_b is the rated capacity of the battery in Ah.

IV. HYBRID CONTROL OF DC-DC CONVERTER

The DC-DC converter includes discrete dynamics due to the switching nature and continuous dynamics. This can be modeled based on hybrid dynamical systems with differential equations and inclusions with constraints as explained in [9] as:

$$\mathcal{H} = \begin{cases} \dot{x} = f(x) & x \in \mathcal{C} \\ x^+ = g(x) & x \in \mathcal{D} \end{cases} \quad (10)$$

where $x = [v_p \ v_b \ v_{dc} \ i_{dcv} \ q \ \tau]^T$. Then, the flow map $f(x)$, jump map $g(x)$, flow set \mathcal{C} and jump set \mathcal{D} can be defined as:

$$\begin{aligned} f(x) &:= \begin{pmatrix} \frac{1}{C_p} \left(-\frac{v_p}{R_p} - \frac{v_p + v_{oc} - v_b}{R_o} \right) \\ \frac{1}{C_p} \left(\frac{v_p + v_{oc} - v_b}{R_o} - i_{dcv} \right) \\ \frac{1}{C_{dc}} (i_{dc,1} + i_{dc,2} + qi_{dcv} - \frac{P_M}{v_{dc}}) \\ \frac{1}{L_b} (v_b - qv_{dc}) \\ 0 \\ 1 \end{pmatrix} \\ g(x) &:= \begin{pmatrix} x_1 \\ x_2 \\ x_3 \\ x_4 \\ \begin{cases} 1 & \text{if } i_{dcv} > i_{dcv}^* \\ 0 & \text{if } i_{dcv} \leq i_{dcv}^* \end{cases} \\ 0 \end{pmatrix} \end{aligned} \quad (11)$$

$$\begin{aligned} \mathcal{C} &:= \{\mathbb{R}^2 \times [900, 1100] \times [-1000, 1000] \times \{0, 1\} \times [0, T_{sw}]\} \\ \mathcal{D} &:= \{\mathbb{R}^2 \times [900, 1100] \times [-1000, 1000] \times \{0, 1\} \times \{T_{sw}\}\} \end{aligned} \quad (12)$$

where τ is a timer, so the status of the switches should be kept opened or closed until the time reaches to the switching time T_{sw} as defined in Table. II. v_{dc} and i_{dcv} are compact set because of droop controller and C-rate limitation each.

To verify the nominal well-posedness of the hybrid system, hybrid basic conditions should be satisfied as explained in [9]:

- 1) \mathcal{C} and \mathcal{D} are closed subsets of \mathbb{R}^n
- 2) $f : \mathbb{R}^n \Rightarrow \mathbb{R}^n$ is outer semicontinuous and locally bounded relative to \mathcal{C} , $\mathcal{C} \subset \text{dom } f$, and $f(x)$ is convex for every $x \in \mathcal{C}$
- 3) $g : \mathbb{R}^n \Rightarrow \mathbb{R}^n$ is outer semicontinuous and locally bounded relative to \mathcal{D} , and $\mathcal{D} \subset \text{dom } g$

Based on \mathcal{C} , $f(x)$ is differentiable and continuous, so $f(x)$ can be identified with a hybrid system satisfying hybrid basic conditions above [9].

V. STABILITY ANALYSIS

The proposed Lyapunov function candidate can be chosen to ensure the stability of v_{dc} and the performance of i_{dcv} as:

$$V(x) := (z - z^*)^T P (z - z^*) \quad (13)$$

where $z = [v_{dc} \ i_{dcv}]^T$ and $P = \begin{bmatrix} p_{11} & 0 \\ 0 & p_{22} \end{bmatrix} > 0$. The reduced states are used in $V(x)$ as z , because the stabilities of the other states are ensured by their own controllers or itself. For example, in the equations of the AC system, the assumption is that the AC source as a pure sinusoidal wave can ensure the stability because the voltage can be supplied constantly regardless of the system condition. Likewise, the battery states are also stable due to its constant voltage supply by v_{ocv} , so only v_{dc} and i_{dcv} are chosen as the states of interest, since they can be influenced by the DC-DC converter control. Then, the relaxed Lyapunov conditions (the strict decrease assumptions are weakened) are used for the uniform global pre-asymptotic stability for a compact set $\mathcal{A} = [v_p^* \ v_b^* \ v_{dc}^* \ i_{dcv}^* \ q^* \ \tau^*]^T$ based on Proposition 3.24 and 3.27 in [9] as:

- 1) $V(x)$ should be continuously differentiable on a neighborhood of \mathcal{C} and continuous on \mathcal{D}
- 2) $V(x) = 0, \forall x \in \mathcal{A} \cap (\mathcal{C} \cup \mathcal{D})$
- 3) $V(x) > 0, \forall x \in (\mathcal{C} \cup \mathcal{D}) \setminus \mathcal{A}$
- 4) The subsets $\{x \in \mathcal{C} \cup \mathcal{D} : V(x) \leq C\}$ should be compact
- 5) $\langle \nabla V(x), f(x) \rangle \leq 0, \forall x \in \mathcal{C}, f(x) \in f$
- 6) $V(g(x)) - V(x) \leq 0, \forall x \in \mathcal{D}, g(x) \in g$

The conditions (1) to (4) can be satisfied because the Lyapunov function candidate is a quadratic function. For the condition (5), the inner product between the gradient of V and the directions along with reduced order flow map $f(x)$ is computed as:

$$\begin{aligned} \langle \nabla V(x), f(x) \rangle = & \\ & 2p_{11}(v_{dc} - v_{dc}^*) \left(\frac{1}{C_{dc}} (i_{dc,1} + i_{dc,2} + q i_{dcv} - \frac{P_M}{v_{dc}}) \right) \\ & + 2p_{22}(i_{dcv} - i_{dcv}^*) \left(\frac{1}{L_b} (v_b - q v_{dc}) \right) \end{aligned} \quad (14)$$

Then, according to q , (14) should be computed and compared as:

$$\arg \max_{q \in \{0,1\}} \langle \nabla V(x), f(x) \rangle \leq 0 \quad (15)$$

When q is zero, (14) can be simplified as:

$$\langle \nabla V(x), f(x) \rangle_{q=0} = \frac{2p_{22}}{L_b} (i_{dcv} - i_{dcv}^*) v_b \quad (16)$$

where $i_{dc,1} + i_{dc,2} - \frac{P_M}{v_{dc}} = 0$ because of the power balance assuming that v_{dc} is constant during the switching period (T_{sw}) of the DC-DC converter. If the control law is selected such that q is zero when $i_{dcv} < i_{dcv}^*$ while $v_b > 0$, $\langle \nabla V(x), f(x) \rangle_{q=0} \leq 0$ can be satisfied.

$$\begin{aligned} \langle \nabla V(x), f(x) \rangle_{q=1} = & \\ & \frac{2p_{11}}{C_{dc}} (v_{dc} - v_{dc}^*) (i_{dc,1} + i_{dc,2} + i_{dcv} - \frac{P_M}{v_{dc}}) \\ & + \frac{2p_{22}}{L_b} (i_{dcv} - i_{dcv}^*) (v_b - v_{dc}) \end{aligned} \quad (17)$$

Similarly, for the case of $q = 1$ in (17), the first term becomes zero due to the power balance, and the control law is selected such that q is unity when $i_{dcv} > i_{dcv}^*$ while $v_b > 0$.

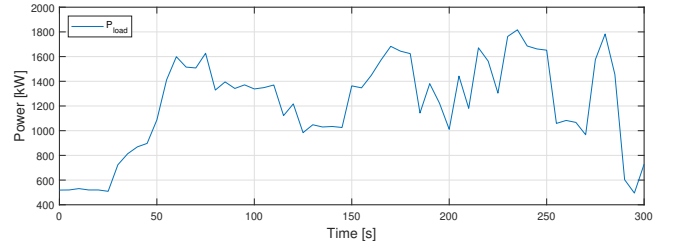


Fig. 4. Load profile for the simulation

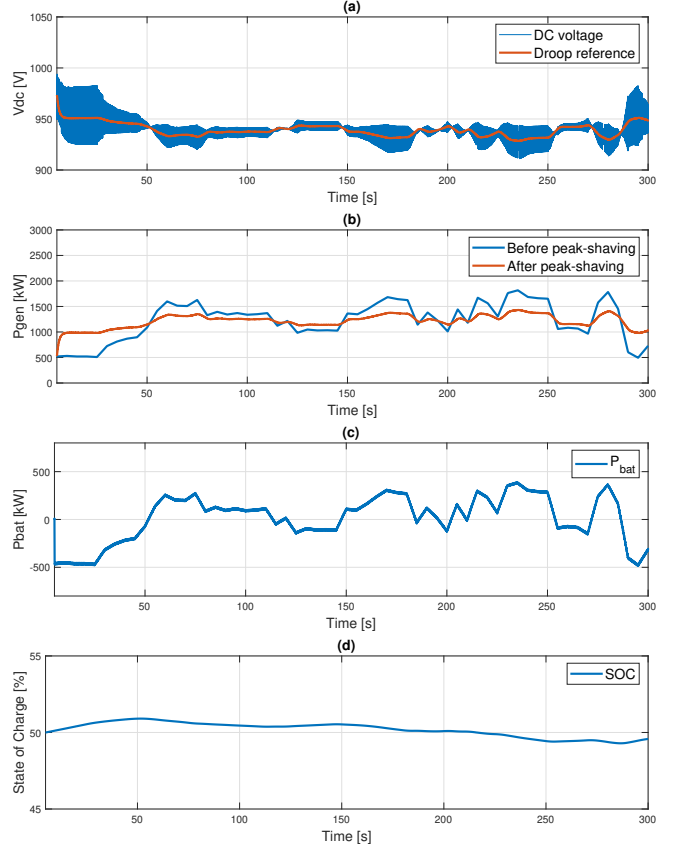


Fig. 5. Simulation results for the peak-shaving via hybrid control (a) DC bus voltage (b) Supplied power of the DGs (c) Battery power (d) Battery SOC

Then, $\langle \nabla V(x), f(x) \rangle_{q=1} \leq 0$ can be satisfied as well. Even though it is not balanced with i_{dcv} (i.e. $i_{dc,1} + i_{dc,2} = \frac{P_M}{v_{dc}}$), very small p_{11} can be always found because v_{dc} and i_{dcv} are bounded while the second term is less than and not equal to zero.

For the stability condition (6), the values of the Lyapunov candidate before and after the jump are the same because q is not included in the function.

$$V(x^+) - V(x) = 0 \leq 0 \quad (18)$$

Therefore, the stability condition (6) can be also satisfied. Therefore, the control law of q in (11) is verified with the stability analysis.

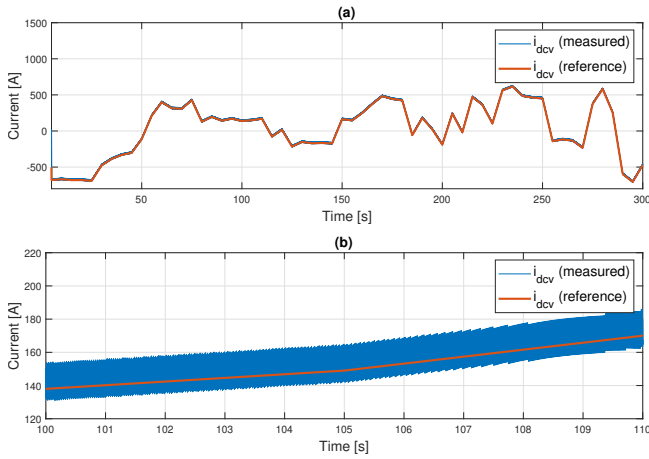


Fig. 6. The results of the hybrid control (a) The current through the inductor in the DC-DC converter (b) Magnified graph of (a)

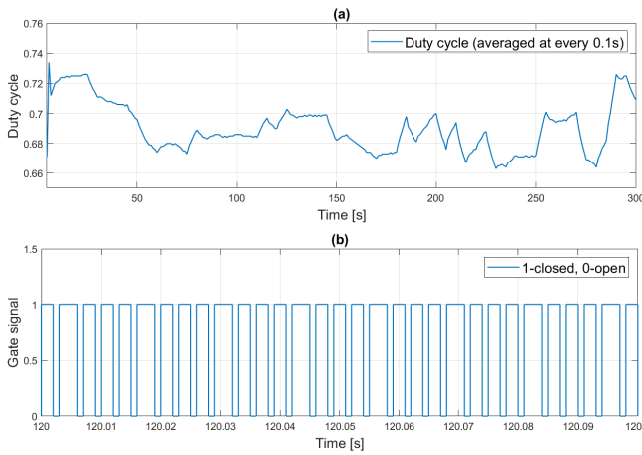


Fig. 7. Hybrid control of the DC-DC converter (a) Duty cycle of q (b) Switching status of q

VI. RESULTS AND DISCUSSIONS

In this section, the simulation models are established for the dynamic analysis of the system. To verify the proposed control method, the load profile as shown in Fig. 4 is prepared, which represents a high transient maneuvering ship operation in order to check the peak-shaving performance clearly.

It is assumed that the best efficiency set-point of the DGs is 1200 kW for a given time period, and the remaining positive or negative required power becomes the reference current of i_{dcv} (i.e. $i_{dcv,ref}$). In addition, the droop coefficient is chosen as 10% in order to observe the effect of the droop control more clearly in the result.

In Fig. 5 (a), it is observed that the DC voltage fluctuations come from the switching effect of the DC-DC converter, but the fluctuation occurs within the acceptable range along with the voltage reference by droop control. The performance of the peak-shaving is well described in Fig. 5 (b).

The supplied power of the DGs is more centered near the

reference value at 1200 kW by the hybrid control of the DC-DC converter as shown in 5 (c). Since the battery has a cyclic operation in its power by charging and discharging, SOC can remain nearly constant at the initial value (50 %). This can be beneficial to the increased lifetime of the battery.

Since the battery output voltage is relatively constant due to the constant v_{ocv} , the current output is alike to the power output of the battery. The measured current output follows the reference as shown in Fig. 6 (a) and (b) by the switching operation of the switches via hybrid control. The duty cycle of this switching operation (q) is averaged at every 0.1s in Fig. 7 (a), and Fig. 7 (b) shows that the hybrid control results in the variable switching frequency of the DC-DC converter over time.

VII. CONCLUSION

In this study, it is demonstrated how hybrid control can be applied to the bidirectional DC-DC converter in order to control the power of the battery for the peak-shaving. The Lyapunov-based stability analysis ensures the proposed switching law not to cause instability in the system, especially in v_{dc} . The results show that the proposed control method does not impact the voltage fluctuations to the unacceptable level. In addition, hybrid control does not include the integral calculation in switching control compared to PI control as a conventional method, so it has an advantage of the less computational workload over the PI control method. Also, the result shows that the peak-shaving operation can increase the lifetime of the battery by decreasing cyclic operation in terms of its SOC change.

REFERENCES

- [1] H. Alafnan, M. Zhang, W. Yuan, J. Zhu, J. Li, M. Elshiekh, and X. Li, "Stability improvement of DC power systems in an all-electric ship using hybrid SMES/battery," *IEEE Trans. Applied Superconductivity*, vol. 28, no. 3, pp. 1–6.
- [2] T. I. Bø and T. A. Johansen, "Battery power smoothing control in a marine electric power plant using nonlinear model predictive control," *IEEE Trans. Control Systems Technology*, vol. 25, no. 4, pp. 1449–1456.
- [3] P. Ghimire, D. Park, M. K. Zadeh, J. Thorstensen, and E. Pedersen, "Shipboard electric power conversion: System architecture, applications, control, and challenges [technology leaders]," *IEEE Electrification Magazine*, vol. 7, no. 4, pp. 6–20.
- [4] T. A. F. Theunisse, J. Chai, R. G. Sanfelice, and W. P. M. H. Heemels, "Robust Global Stabilization of the DC-DC Boost Converter via Hybrid Control," *IEEE Trans. Circuits and Systems I: Regular Papers*, vol. 62, no. 4, pp. 1052–1061, Apr. 2015.
- [5] U. Javaid, F. D. Freijedo, D. Dujic, and W. v. d. Merwe, "MVDC supply technologies for marine electrical distribution systems," *CPSS Trans. Power Electronics and Applications*, vol. 3, no. 1, pp. 65–76.
- [6] K. Areerak, S. V. Bozhko, G. M. Asher, and D. W. P. Thomas, "Stability analysis and modelling of AC-DC system with mixed load using DQ-transformation method," in *2008 IEEE International Symposium on Industrial Electronics*, pp. 19–24.
- [7] M. Sakui, H. Fujita, and M. Shioya, "A method for calculating harmonic currents of a three-phase bridge uncontrolled rectifier with DC filter," *IEEE Trans. Industrial Electronics*, vol. 36, no. 3, pp. 434–440.
- [8] S. M. Mousavi G. and M. Nikdel, "Various battery models for various simulation studies and applications," *Renewable and Sustainable Energy Reviews*, vol. 32, pp. 477–485.
- [9] R. Goebel, R. G. Sanfelice, and A. R. Teel, *Hybrid dynamical systems: modeling, stability, and robustness*. Princeton University Press.